THE JOURNAL OF PHYSICAL CHEMISTRY A

Article

pubs.acs.org/JPCA

Identification of the Strongest Bonds in Chemistry

Robert Kalescky, Elfi Kraka, and Dieter Cremer*

Department of Chemistry, Southern Methodist University, 3215 Daniel Avenue, Dallas, Texas 75275-0314, United States

Supporting Information

ABSTRACT: Increasing the effective electronegativity of two atoms forming a triple bond can increase the strength of the latter. The strongest bonds found in chemistry involve protonated species of hydrogen cyanide, carbon monoxide, and dinitrogen. CCSD(T)/CBS (complete basis set) and G4 calculations reveal that bond dissociation energies are misleading strength descriptors. The strength of the bond is assessed via the local stretching force constants, which suggest relative bond strength orders (RBSO) between 2.9 and 3.4 for heavy atom bonding (relative to the CO bond strength in methanol (RBSO = 1) and formaldehyde (RBSO = 2)) in $[HCNH]^+(^1\Sigma^+)$, $[HCO]^+(^1\Sigma^+)$, $[HNN]^+(^1\Sigma^+)$, and $[HNNH]^{2+}(^1\Sigma_g^+)$. The increase in strength is caused by protonation, which increases the electronegativity of the heavy atom and thereby decreases the energy of the bonding AB orbitals (A, B: C, N, O). A similar effect can be achieved by ionization of a nonbonding or antibonding electron in CO or NO. The strongest bond with a RBSO value of 3.38 is found for $[HNNH]^{2+}$ using scaled CCSD(T)/CBS frequencies determined for CCSD(T)/CBS geometries. Less strong is the NN bond in $[FNNH]^{2+}$ and $[FNNF]^{2+}$.

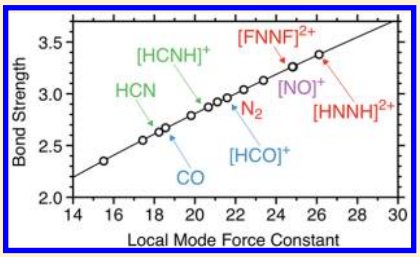

1. INTRODUCTION

Pauling,[1] Slater,[2] and Mulliken[3] pioneered our understanding of the chemical bond according to which the strength of a bond depends on the degree of overlap between the interacting atomic orbitals and the bond polarity reflected by the difference in the energies of the atomic orbitals involved in bonding. In a simplified form, one can say that the bond strength is influenced by covalent (overlap) and ionic effects (bond polarity). The strongest bonds measured in terms of their bond dissociation enthalpies (BDH)[4] are found between elements of the second period of the periodic table (Figure 1). This is a result of the fact that, for this period, the flexibility in orbital hybridization makes triple bonds possible. A σ bond is formed by sp−sp overlap and complemented by two π-bonds of similar strengths, which in total almost triples the BDH of a single bond as shown for the pairs acetylene−ethane, hydrogen cyanide−methylamine, dinitrogen−hydrazine, or carbon monoxide−methanol in Figure 1.[4,5]

HC≡CH	HC≡N	N≡N	C≡O
228.0	223.4	225.8	257.3
$H_2C{=}CH_2$		HN=NH	$H_2C{=}O$
174.1		119.7	180.6
$H_3C{-}CH_3$	$H_3C{-}NH_2$	$H_2N{-}NH_2$	$H_3C{-}OH$
90.2	85.1	66.2	92.0
$H_2Si{=}SiH_2$	P≡P	Si≡O	C≡S
27.0	116.9	191.1	106.8
Si=C	P≡N	Ge≡O	Si≡S
106.8	147.5	157.8	147.9
$H_3Si{-}F$	As≡As	Sn≡O	
152.5	92.2	126.3	
$F_3Si{-}F$	As≡N	Pb≡O	
166.6	116.9	89.4	

Figure 1. Comparison of measured bond dissociation enthalpies (BDHs).[4]

For elements of the third and higher periods, hybridization is largely absent and π-bonds are much weaker than the corresponding σ-bonds.[5,6] Accordingly, the triple bonds are in total much weaker than those between elements of the second period, which is reflected by measured BDH values of suitable examples shown in Figure 1.[4] The P_2 and As_2 molecules have BDH values, which are just 52% and 41% as large as that of N_2. For PN and AsN, somewhat larger values were measured (65% and 52% of BDH(N_2)); however, they are still substantially smaller than typical BDH values of the second period examples. Similar trends are observed for the higher period homologues of CO: With increasing atomic number and increasing covalent radius, overlap is reduced and the π-bonds become significantly weaker.[4,5] An increase in the bond strength can be enforced by increasing the bond polarity in molecules such as $H_3Si{-}F$ or $F_3Si{-}F$ (Figure 1); however, the corresponding BDHs are still far below the highest values observed for the second period atoms linked by triple bonds.

Apart from these two distinct possibilities of increasing the bond strength (increase of overlap and increase of the bond polarity), a third possibility is suggested by molecular orbital (MO) theory: If for a triple-bonded molecule A≡A or A≡B, the effective electronegativity of A (and B) is increased, the energies of the atomic valence orbitals and the bonding orbital(s) are lowered, thus leading to a strengthening of the bond. The BDH

Received: June 23, 2013
Revised: August 8, 2013
Published: August 8, 2013

dx.doi.org/10.1021/jp406200w | J. Phys. Chem. A 2013, 117, 8981−8995

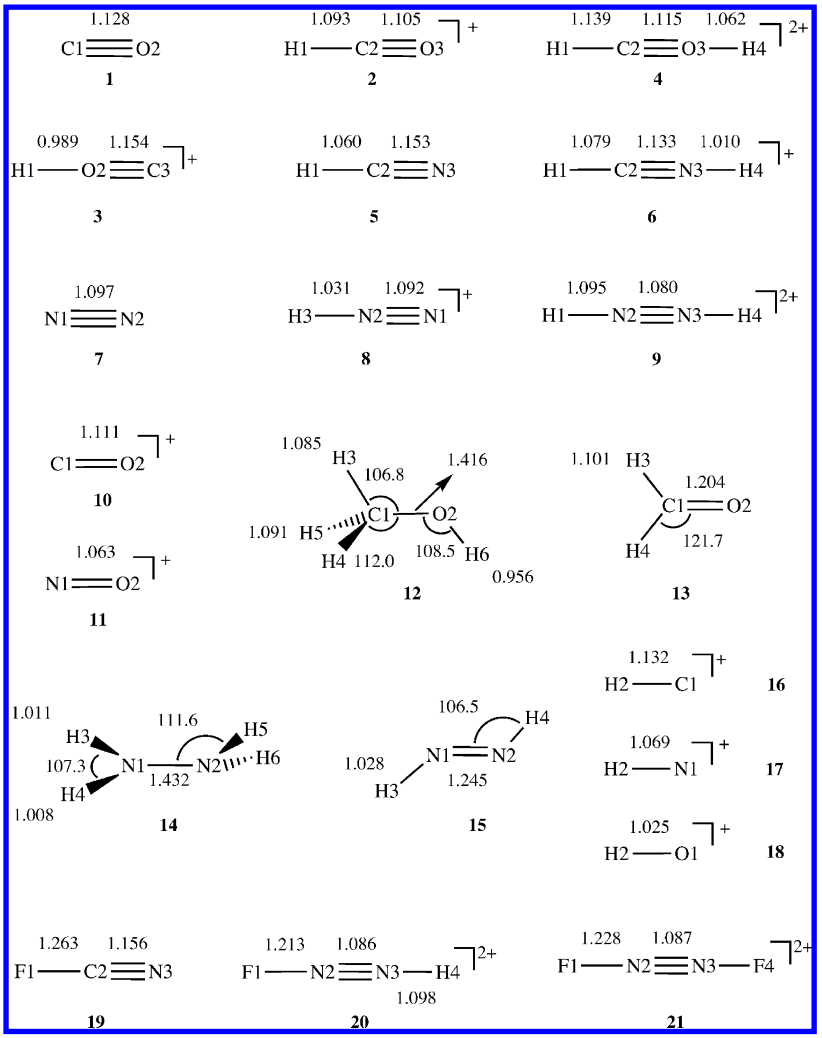

Figure 2. CCSD(T)/CBS geometries of the molecules **1**−**21**. Bond lengths in Å and angles in deg. The numbering of atoms is indicated.

values of acetylene and molecular nitrogen do not reflect this trend (228.0 and 225.8 kcal/mol;[4] Figure 1), which indicates what we will discuss in the following: *BDH (or bond dissociation energies, BDE) values, although often used in chemistry to discuss the strength of the chemical bond,[4,7] are not reliable bond strength descriptors.*

According to measured BDH values, carbon monoxide should have the strongest triple bond of all second period molecules (257.3 kcal/mol;[4] Figure 1) where of course this may also be misleading. In this work, we will discuss which of the triple bonds shown in the first row of Figure 1 is the strongest and how the strength of these triple bonds can be in general increased by increasing the effective electronegativity of the atoms participating in the bond. A possibility of increasing the effective electronegativity of atoms A or B is the substitution by electronegative substituents such as F. For example, FC≡CF should possess a stronger triple bond than HC≡CH.

An even more effective way of increasing the electronegativity of the atoms A and B connected by a triple bond is to introduce positive charges at A and/or B, however, without reducing the number of electrons participating in the triple bond. This implies that A and/or B possess electron lone pairs, which, for example, are converted into bonding electron pairs via protonation of A and/or B. The lone pair orbitals should be of the σ-type (oriented away from the triple bond) to avoid, in the case of a double protonation, a weakening of the existing triple bond by charge repulsion as much as possible. Hence, potential candidates for an electronegativity-driven strengthening of an existing triple bond would be the protonated or double-protonated N≡N or C≡O and the protonated HC≡N, which are all isoelectronic with the acetylene molecule (Figure 1).

An electronegativity-driven strengthening of a triple bond will also be effective for triply bonded molecules involving third and higher period atoms (Figure 1). However, because the triple-bond strength of the neutral molecule is much smaller in these cases, for the reasons discussed above, there will not be any chance of getting a bond stronger than to be expected from a protonated second period molecule with triple bond. (For a discussion of triple bonds and their typical length, see Pyykkö and co-workers.[8])

In this work, we will investigate the question of how to obtain the strongest bond possible in chemistry using the electronegativity principle discussed above. This will include a comparison of the bond strengths of typical second row molecules with triple bonds and their analogues with increased electronegativity of A and/or B. Our target samples are shown in Figure 2. They comprise protonated forms of C≡O, HC≡N, and N≡N. In connection with the discussion of the strength of the heavy atom bond in these molecules, we will demonstrate that the BDH (BDE) values are always influenced by the relative

dx.doi.org/10.1021/jp406200w | J. Phys. Chem. A 2013, 117, 8981−8995

stability of the dissociation fragments.[9] We will, instead of using BDHs (BDEs), refer to local stretching modes and their force constants, which provide a reliable dynamic measure of the bond strength.[10−14]

The results of this work will be presented as follows. In Section 2, the theoretical methods used in this work will be described. Results and Discussion will be presented in 3, and the last section will be devoted to the conclusions that can be drawn from this investigation.

2. COMPUTATIONAL METHODS

The description of the chemical bond with the help of stretching force constants dates back to the 1920s and 1930s when Badger[15] found relationships between force constant and bond length for diatomic molecules.[13] The extension of these relationships to polyatomic molecules turned out to be problematic because spectroscopically derived stretching force constants are not unique, reflect mode−mode coupling, and depend on the internal coordinates used for the description of a molecule.[13]

Decius[16] and others[17,18] solved this problem by reverting to the inverse force constant matrix and introducing the compliance constants as coordinate independent bond strength descriptors. Ample work has been carried out with the compliance constants to describe the properties of chemical bonds[19−21] although their physical meaning and relationship to the normal vibrational modes remained unclear. McKean[22−24] solved the problem of obtaining reliable stretching force constants by measuring *isolated* XH stretching frequencies for a suitable isotopomer of a given target molecule where the 2:1 mass ratio of deuterium to hydrogen was exploited to obtain XH stretching frequencies and force constants of mass-decoupled local vibrational modes. Henry[25] pioneered the technique of obtaining local mode information from overtone spectra. Apart from this, there were numerous attempts to set up relationships between stretching force constants or frequencies and bond strength descriptors such as BDE values, bond orders, bond lengths, etc., which are discussed in a 2010 review article that underlines the necessity of obtaining local mode information from normal vibrational modes.[13]

In 1998, the physical basis for deriving local vibrational modes directly from normal vibrational modes was presented by Konkoli and Cremer.[26] However, it took more than 10 years to prove that the Konkoli−Cremer modes are unique and the only local modes that relate directly to the normal modes when the basic equations of vibrational spectroscopy are solved.[10,11] Local vibrational modes are determined according to Konkoli and Cremer by solving the mass-decoupled Euler−Lagrange equations.[26] Each local mode is associated with an internal coordinate q_n ($n = 1, ..., N_{vib}$ with $N_{vib} = 3N - L$; N is the number of atoms; L is the number of translations and rotations) used to describe the geometry of the molecule in question. It is related to the normal vibrational modes of the molecule by[26]

$$\mathbf{a}_n = \frac{\mathbf{K}^{-1}\mathbf{d}_n^{\dagger}}{\mathbf{d}_n\mathbf{K}^{-1}\mathbf{d}_n^{\dagger}} \tag{1}$$

where $\mathbf{K}$ is the diagonal matrix containing the force constants k_μ of the normal vibrational modes $\mathbf{d}_\mu$ ($\mu = 1, ..., N_{vib}$) expressed also in terms of internal coordinates:

$$\mathbf{K} = \mathbf{D}^{\dagger}\mathbf{F}^{q}\mathbf{D} \tag{2}$$

which is obtained by solving the vibrational eigenvalue problem, i.e., the Wilson equation:[27]

$$\mathbf{F}^{q}\mathbf{D} = \mathbf{G}^{-1}\mathbf{D}\mathbf{\Lambda} \tag{3}$$

Here, $\mathbf{F}^q$ is the force constant matrix expressed in internal coordinates q_n, $\mathbf{D}$ collects the vibrational eigenvectors $\mathbf{d}_\mu$ in form of column vectors, $\mathbf{G}$ is the Wilson $\mathbf{G}$-matrix,[27] and $\mathbf{\Lambda}$ is a diagonal matrix containing the vibrational eigenvalues $\lambda_\mu = 4\pi^2c^2\omega_\mu{}^2$ where ω_μ represents the (harmonic) vibrational frequency of normal mode $\mathbf{d}_\mu$.

Once the vibrational eigenvalue problem is solved, matrix $\mathbf{K}$ and the row vectors $\mathbf{d}_n$ of matrix $\mathbf{D}$ can be determined to derive local mode vectors $\mathbf{a}_n$. These in turn are sufficient to calculate local mode force constants k_n^a and local mode frequencies ω_n^a according to[26]

$$k_n^a = \mathbf{a}_n^{\dagger}\mathbf{K}\mathbf{a}_n = (\mathbf{d}_n\mathbf{K}^{-1}\mathbf{d}_n^{\dagger})^{-1} \tag{4}$$

and

$$\omega_n^a = \sqrt{k_n^a G_{nn}} \tag{5}$$

where G_{nn} is a diagonal element of the Wilson $\mathbf{G}$-matrix.

The local vibrational modes have a number of advantages: (i) A local mode depends only on the internal coordinate it is associated with (*leading parameter principle*[26]) and is independent of all other internal coordinates used to describe the geometry of a molecule. Accordingly, it is also independent of using redundant or nonredundant coordinate sets. (ii) The local modes confer physical meaning to the compliance constants Γ_n of Decius.[16] Zou and co-workers[10,11] have proved that $1/\Gamma_n = k_n^a$; i.e., the reciprocal of the compliance constants are equal to the local mode force constants and thereby the compliance constants can be associated with a physically well-defined mode and its properties. (iii) As was shown by Cremer and co-workers, local mode frequencies and force constants can be determined from a complete set of $3N - L$ measured fundamental frequencies utilizing perturbation theory.[12] In this way, one can distinguish between calculated harmonic local mode frequencies (force constants) and experimentally based local mode frequencies (force constants), which differ by anharmonicity effects.[28,29] (iv) Konkoli and Cremer have shown that each normal vibrational mode can be characterized in terms of local vibrational modes, where their Characterization of Normal Mode (CNM) method is superior to the potential energy distribution analysis.[13,30]

Local mode frequencies can be related to normal-mode frequencies in an adiabatic connection scheme (ACS), which reveals the kinematic coupling mechanism between the local modes such that the results of the CNM analysis can be physically explained.[10,11] In this work, the ACS of all polyatomic molecules have been determined to verify the results of the CNM analysis.

For molecules **1**−**21** (Figure 2), geometries and harmonic vibrational frequencies were calculated using Dunning's aug-cc-pVDZ, aug-cc-pVTZ, and aug-cc-pVQZ basis sets.[31] These calculations were the basis for extrapolating results to the complete basis set (CBS) limit employing a three-point extrapolation formula.[32,33] The CCSD(T)/CBS harmonic vibrational frequencies were then used to determine the corresponding CCSD(T)/CBS local mode frequencies and force constants as well as the ACS diagrams defining CCSD(T)/CBS coupling frequencies.[10,11,28,29]

In cases where experimental frequencies are available (CO,[34] $[HCO]^+$,[35] HCN,[36] $[HCNH]^+$,[37−41] NN,[42] $[CO]^+$,[43] $[NO]^+$,[43] CH_3OH,[44] H_2CO,[44] H_2NNH_2,[45] *t*-HNNH,[46] $[HC]^+$, $[NH]^+$, $[OH]^+$,[43] FCN[47]), these frequencies were used to determine a set of scaling factors (Table 1) to convert harmonic vibrational

dx.doi.org/10.1021/jp406200w | J. Phys. Chem. A 2013, 117, 8981−8995

Table 1. Scaling Factors for CCSD(T)/CBS Harmonic Frequencies Used in This Work[a]

target molecule	reference molecule	vibration type	scaling factor
$[COH]^+$	**2**, **1**, **13**	CO stretch	0.9815
	1, **12**	OH stretch	0.9495
	12	HOC bend	0.9600
$[HNN]^+$ and $[HNNH]^{2+}$	**7**, **1**	NN stretch	0.9856
	15	NH stretch	0.9469
	15	HNN bends	0.9766
$[HCNH]^+$	**5**	CN stretch	0.9821
	5	HC stretch	0.9601
	15	NH stretch	0.9469
	5	HCN, CNH bends	0.9442
$[FNNH]^{2+}$ and $[FNNF]^{2+}$	**1**, **7**, **19**	FN stretch	0.9809
	1, **7**, **19**	FNN bend	0.9686

[a]Compare with Figure 2 and Tables 2 and 4.

frequencies obtained at the CCSD(T)/CBS level into reliable normal-mode frequencies in all those cases where experimental frequencies are not available. In previous work, we have shown that by mode-specific scaling of CCSD(T)/CBS frequencies, accurate normal-mode frequencies can be obtained, which are more reliable than frequencies obtained with anharmonicity corrections.[28] The scaling factors were tested for $[HCNH]^+$: The average deviation between CCSD(T)/CBS and experimental frequencies is 79 cm^{-1}. With the scaling factors of Table 1, the average deviation could be reduced to 14 cm^{-1}. For the experimental and the scaled harmonic frequencies, the perturbation approach described by Cremer and co-workers was used to derive *experimental* (=experimentally based) local mode frequencies and force constants.[12]

The local mode stretching force constants provide reliable bond strength descriptors,[10−14,28,29] which for the purpose of facilitating the analysis, can be converted into bond orders if bonds of the same type are compared or relative bond strength orders (RBSO) if different types of bonds are compared. As described in previous work,[48,49] we used the single and double CO bonds in methanol and formaldehyde with a bond order n = 1 and 2, respectively, as reference, a power relationship between bond order (or RBSO) and stretching force constants, and the requirement that for $k^a = 0$ the bond order n is also equal to zero. Badger[15] has shown for diatomic molecules that bonds between atoms of the same period all follow similar k−r relationships (r: bond length). Kraka and co-workers have extended the Badger rule to polyatomic molecules utilizing the local stretching force constants and substituting for the bond length r the bond order or RBSO n.[13,14] According to their results, a generalized and extended Badger rule can be formulated: *Different bonds between atoms of the same period can be described by one common power relationship relating local mode stretching force constants to bond orders or RBSOs as suitable bond strength descriptors.*

Hence, different bond types AB can be described with one force constant-bond order relationship if bonds between second period atoms are considered. This was used to determine the different bond orders of CF bonds with the help of suitable CO references[48] and the RBSO values of different XH bonds using FH (n = 1.0)[43] and $[F\cdots H\cdots F]^-$ (n = 0.5)[50] as reference bonds.[28,29,49]

In this work, we extend this approach to CN and NN bonds. RBSO values chosen in this way reflect the change in bond strength when a CO bond is replaced, for example, by a CF bond. Within a group of molecules possessing CF bonds, one can simplify the discussion by introducing an additional reference bond (e.g., the C−F bond in H_3C−F as a new standard bond with n = 1.0) and scale calculated bond orders to this additional reference. We have done this by using the XH bond in methane, ammonia, and water as standard single bonds with n = 1.0 for C−H, N−H, or O−H. Both direct RBSO values and scaled bond orders are given. Furthermore, we give RBSO values based on CCSD(T)/CBS harmonic frequencies and measured (scaled) frequencies. They lead to equivalent descriptions of the bond strength. We will discuss the RBSO values based on experimental or scaled frequencies as, in this way, possible insecurities in relative bond strength parameters caused by anharmonicity effects are eliminated.

The term bond order is usually applied in connection with MO descriptions and their population analysis. On this basis, the bond orders of acetylene and dinitrogen are both about 3 although the CC and NN bond have a different bond strength;, i.e., the bond order is simply a counter for the number of bonding interactions without quantifying the bond strength. In this work, the RBSO index is introduced as a parameter, which quantifies the strength of a bond in relationship to a suitable reference bond. If the strength is discussed for the same bond type including two suitable reference bonds, then use of the term bond order will be justified, Otherwise, the term RBSO is suitable.

The approach of describing the bond strength via the local mode stretching force constant is based on features of the adiabatic Born−Oppenheimer potential energy surface (PES) as it is described by measured or calculated spectroscopic constants. Hence, in all those cases where the Born−Oppenheimer approximation is no longer valid as, e.g., in the case of nonadiabatic effects, the local mode description based on the adiabatic PES can no longer be applied. However, for all molecules being discussed in this work, the adiabatic Born−Oppenheimer PES provides a reasonable description of molecular features close to the equilibrium geometry.

Apart from this, we have to make a caveat with regard to other potential shortcomings of the local mode description of the bond strength: (i) The Wilson equation does not provide a quantum mechanical description of vibrating molecules. (ii) Measured vibrational frequencies preferentially used in this work might be erroneous. (iii) The derivation of vibrational force constants from measured vibrational frequencies is based on a perturbational approach and therefore leads to errors up to 1−2% in the calulated local mode frequencies.[12] (iv) When measured frequencies are not available, vibrational frequencies have to be calculated using the harmonic approximation. Hence, the accuracy of the computed frequencies depends on the method and basis set used, the calculation of anharmonicity corrections or the availability of reliable scaling factors. This last effect has clearly the largest impact on the predicted RBSO values, and therefore, experimental frequencies or carefully scaled CCSD(T)/CBS frequencies have been used throughout this work.

The bond dissociation energies (BDE; values include zero-point energies) and bond dissociation enthalpies at 298.15 K (BDH(298)) were calculated for the target molecules using the Gaussian-4 (G4) method.[51] The G4 method provides reliable BDE and BDH values, which are comparable to experimental results. In some cases, we investigated different dissociation channels to demonstrate the influence of excited state energies on the BDE or BDH value. The G4 method becomes unreliable when the dissociating molecule and/or the dissociation frag-

dx.doi.org/10.1021/jp406200w | J. Phys. Chem. A 2013, 117, 8981−8995

ments possess multireference character. Because of this, we determined the energy of the O(^{1}D) state via the experimental value of the difference between the ^{3}P and ^{1}D state of atomic oxygen[52] and the energy of N(^{2}D) via the corresponding value between the ^{4}S and ^{2}D state of atomic nitrogen.[53]

The local mode calculations were carried out with the ab initio package COLOGNE2013,[54] all CCSD(T) calculations with the package CFOUR,[55] and the G4 calculations with Gaussian09.[56]

3. RESULTS AND DISCUSSION

In Figure 2, the CCSD(T)/CBS geometries of the molecules investigated in this work are given. CCSD(T)/CBS harmonic vibrational frequencies, measured (and scaled harmonic) frequencies, the corresponding local mode frequencies and force constants, their coupling frequencies, and the calculated RBSO values are listed in Table 2 (target molecules) and Table 3 (reference molecules). In Table S1 of the Supporting Information, an analysis of all normal vibrtional modes in terms of local vibrational modes is given. Calculated bond dissociation energies (BDEs), BDH values, and the energies of the proton dissociation reactions are given in Tables 4 and 5 and Figure 3. In the following, we will discuss the strength of triple-bonded molecules and their protonated counterparts.

The difference between CCSD(T)/CBS and experimentally based (scaled) local mode stretching force constants are up to 4%, which is predominantly due to anharmonicity effects. Because these differences are also found for the reference molecules, RBSO values based on CCSD(T)/CBS or experimental (scaled) data differ by 3% or less (Tables 2 and 3). This leads to the important conclusion that the bond strength analysis can be based on calculated harmonic or measured normal-mode frequencies without significantly changing results.

However, the results listed in Tables 2 and 3 (see all Table S1, Supporting Information) also reveal that a direct use of those frequencies and associated force constants, which belong to normal modes dominated by the stretching vibration of the targeted bond causes serious errors. The CNM analysis of the normal vibrational modes determines the CO stretching contribution to be 87 (mode 3 of **2**), 98 (mode 3 of **3**), and 70% (mode 5 of **4**), which makes the corresponding force constants no longer comparable. Similarly, the CN stretching contribution is 93 (mode 3 of **5**) and 86% (mode 5 of **6**), whereas the NN stretching contribution is 90 (mode 3 of **8**), 50 (mode 7 of **9**), 63 (mode 4 of **14**), and 92% (mode 4 of **15**; see Table S1, Supporting Information). Clearly, the properties of the normal modes cannot provide any insight into the strength of the corresponding bond because they are mixtures of local modes with varying stretching contributions.

This conclusion can directly be drawn from the coupling frequencies ω_{coup} listed in Tables 2 and 3 as they provide a measure of the magnitude of mode−mode coupling. These values vary between 36 and 349 cm^{-1}, which makes it impossible to accurately assess the strength of a bond directly from the normal-mode frequencies and their associated force constants. This problem is solved when local vibrational modes are analyzed, and therefore, we will discuss in the following local stretching force constants and RBSO values based on experimental (or scaled harmonic) data preferentially.

Typical Triple Bonds A≡B: Which Bond Is Stronger? MO theory predicts for CO a triple bond when the number of occupied antibonding MOs is formally subtracted from the number of occupied bonding MOs. This conceptual description of the carbon monoxide bond does not consider the magnitude of overlap and the bond polarity in any quantitative sense and therefore is of limited value.

The RBSO based on the stretching force constants of carbon monoxide (CCSD(T)/CBS, harmonic 19.1; experimental 18.5 mdyn/Å, Table 2) and the CO bonds of methanol and formaldehyde as suitable references (Table 3) leads to a bond multiplicity of 2.62 and 2.67, respectively. Although the BDE or BDH values are not reliable in this connection (as will be discussed in detail below), it is noteworthy that the ratio of the values for CO and CH_3OH (Table 4) as well as for CO and CH_2O are between 2.80 and 2.87, which also suggests that a full triple bond is not established in carbon monoxide. The π-bonds in CO are weaker than the σ-bond, which is a result of less than optimal pπ-pπ overlap.

For HCN ($^1\Sigma^+$), the situation is similar to that observed for CO ($^1\Sigma^+$), as is documented by a CN RBSO of 2.63 (Table 2). Only N_2 ($^1\Sigma_g^+$) has a fully developed triple bond. On the basis of the RBSO-stretching force constant relationship established for methanol and formaldehyde, a RBSO of 3.04 is obtained in this case (Table 2). It is interesting to compare the strength of the NN bond with that of the formal triple bond in HC≡CH. Using experimental frequencies, we obtain a RBSO of n = 2.39 (corresponding to k^a = 15.8 mdyn/Å; n(CH) = 1.14, k^a(CH) = 5.9 mdyn/Å), which clearly shows that the CC triple bond is much weaker than the NN triple bond. This is a direct consequence of the electronegativity difference between N and C atoms (about 0.5 units[57]), which increases the NN bond strength relative to the CC bond by 0.65 RBSO units. Because the electron lonepairs of N influence the NN single, double, and triple bonds in different ways, it is difficult to say whether the difference in the triple bond strengths of NN in molecular nitrogen and acetylene is preferentially due to σ- or π-bonding.

We tested the electronegativity principle of bond strength by comparing the triple bonds in HC≡CH and FC≡CF. For the latter molecule, we obtain a local CC stretching force constant of 17.1 mdyn/Å corresponding to n = 2.52 (CF, 8.2 mdyn/Å, n = 1.45; experimental frequencies[58,59] 2450, 1349, 794, 282, 282, 258 cm^{-1}). Attempts of increasing the bond strength even further by substitution with the more electronegative He^+ or Ne^+ as in $HeCCHe^{2+}$ or $NeCCNe^{2+}$ [60,61] were not successful because the noble gases withdraw electron density from the CC triple bond to strengthen the CHe or CNe bonds. We conclude that FC≡CF possesses one of the strongest, if not the strongest, CC triple bond.

Protonation of Carbon Monoxide. By protonation at C, the electronegativity of the C atom is increased, its covalent radius decreased (bond length decrease from 1.128 to 1.105 Å by 2%, Figure 2), and a stronger bond established. The molecular orbitals retain their overall-nodal structure but are contracted especially at the C side. The calculated BDEs (276.5 kcal/mol, Table 4) suggests a 7% increase whereas the local stretching force constant of 21.6 mdyn/Å (based on the scaled frequencies) indicates a 14% increase, which leads to a RBSO of 2.96, thus presenting, contrary to the neutral molecule, a fully developed triple bond.

The protonation at the O atom has the reverse effect. Although the bond polarity of the CO bond is substantially increased, the contraction of the orbitals at O leads to a mismatch with the atomic orbitals at C and a weakening of the overlap. This is confirmed by the fact that a double protonation of CO and a contraction of the atomic orbitals of both bond atoms causes a strengthening of the CO bond. In the case of $[COH]^+$, the CO bond length is increased by 2% to 1.154 Å and the CO stretching

dx.doi.org/10.1021/jp406200w | J. Phys. Chem. A 2013, 117, 8981−8995

Table 2. CCSD(T)/CBS and Experimental Normal and Local Mode Frequencies Frequencies, ω_μ and ω^a, Local Mode Force Constants, k^a, RBSO Values, n, and Coupling Frequencies, ω_{coup}, for Molecules 1−11 and 19−21

molecule μ	sym	ω_μ^{ha} CBS [cm^{-1}]	ω_μ exp [cm^{-1}]	parameter	κ_{ha}^a CBS [mdyn/Å]	k^a exp [mdyn/Å]	ω_{ha}^a BS [cm^{-1}]	ω^a exp [cm^{-1}]	n^{ha} CBS	n exp	ω_{coup}^{ha} CBS [cm^{-1}]	ω_{coup} exp [cm^{-1}]
1, $CO(^1\Sigma^+)$												
1	Σ	2174.5	2143	O2−C1	19.112	18.554	2174.5	2143.0	2.62	2.67	0.0	0.0
ZPE [kcal/mol]:		3.11	3.06				3.11				0.00	0.00
2, $[HCO]^+(^1\Sigma^+)$												
4	Σ	3252.9	3089	C2−H1	5.362	4.879	3128.7	2984.3	1.01	1.00	124.2	104.4
3	Σ	2225.2	2184	O3−C2	22.584	21.588	2364.5	2311.7	2.93	2.96	−139.3	−127.8
2	Π	862.7	828	O3−C2−H1	0.380	0.350	862.7	828.2			0.0	0.0
1	Π	862.7	828	O3−C2−H1	0.380	0.350	862.7	828.2			0.0	0.0
ZPE [kcal/mol]:		10.30	9.91				10.32	9.94			−0.02	−0.03
3, $[COH]^+(^1\Sigma^+)$												
4	Σ	3467.2	3292	O2−H1	6.629	5.983	3444.8	3272.8	1.18 (0.85)	1.16 (0.84)	22.4	19.3
3	Σ	1959.4	1923	C3−O2	16.121	15.510	1997.7	1959.5	2.33	2.35	−38.3	−36.4
2	Π	142.3	137	C3−O2−H1	0.009	0.009	142.3	136.7			0.0	0.0
1	Π	142.3	137	C3−O2−H1	0.009	0.009	142.3	136.7			0.0	0.0
ZPE [kcal/mol]:		8.16	7.85				8.19	7.87			−0.02	−0.02
4, $[HCOH]^{2+}(^1\Sigma^+)$												
7	Σ	2921.8	2805	C2−H1	3.853	3.565	2652.2	2551.1	0.79	0.79	269.6	254.1
6	Σ	2565.3	2436	H4−O3	3.738	3.401	2586.8	2467.4	0.77 (0.56)	0.76 (0.55)	−21.5	−31.7
5	Σ	2073.7	2035	O3−C2	22.195	21.106	2344	2285.8	2.89	2.92	−270.3	−250.5
4	Π	840.4	807	O3−C2−H1	0.38	0.35	828.6	795.6			11.8	11.2
3	Π	840.4	807	H4−O3−N1	0.38	0.35	828.6	795.6			11.8	11.2
2	Π	530.2	509	O3−C2−H1	0.145	0.134	531.1	509.9			−0.9	−1.0
1	Π	530.2	509	H4−O3−N1	0.145	0.134	531.1	509.9			−0.9	−1.0
ZPE [kcal/mol]:		14.73	14.16				14.73	14.17			0.0	−0.01
5, $HCN(^1\Sigma^+)$												
4	Σ	3448.6	3311	C2−H1	6.218	5.752	3369.2	3240.4	1.13	1.13	79.4	70.6
3	Σ	2135.2	2097	N3−C2	18.958	18.234	2231.4	2188.4	2.60	2.63	−96.2	−91.4
2	Π	754.1	712	N3−C2−H1	0.279	0.249	754.0	712.0			0.1	0.0
1	Π	754.1	712	N3−C2−H1	0.279	0.249	754.0	712.0			0.1	0.0
ZPE [kcal/mol]:		10.14	9.77				10.16	9.80			−0.02	−0.03
6, $[HCNH]^+(^1\Sigma^+)$												
7	Σ	3670.1	3488	H4−N3	7.143	6.448	3590.9	3411.9	1.25 (0.98)	1.22 (0.96)	79.2	76.1
6	Σ	3359.0	3188	C2−H1	5.884	5.327	3277.5	3118.4	1.09	1.06	81.5	69.6
5	Σ	2207.9	2150	N3−C2	21.916	20.656	2399.2	2329.2	2.87	2.87	−191.3	−179.2
4	Π	842.4	802	N3−C2−H1	0.340	0.309	825.1	786.2			17.3	15.8
3	Π	842.4	802	N3−C2−H1	0.340	0.309	825.1	786.2			17.3	15.8
2	Π	673.0	646	H4−N3−C2	0.209	0.193	673.6	646.6			−0.6	−0.6
1	Π	673.0	646	H4−N3−C2	0.209	0.193	673.6	646.6			−0.6	−0.6
ZPE [kcal/mol]:		17.54	16.76				17.53	16.76			0.00	0.00
7, $N_2(^1\Sigma_g^+)$												

dx.doi.org/10.1021/jp406200w | J. Phys. Chem. A 2013, 117, 8981−8995

Table 2. continued

molecule μ	sym	ω_μ^{ha} CBS [cm^{-1}]	ω_μ exp [cm^{-1}]	parameter	κ_{ha}^{a} CBS [mdyn/Å]	k^a exp [mdyn/Å]	ω_{ha}^{a} BS [cm^{-1}]	ω^a exp [cm^{-1}]	n^{ha} CBS	n exp	ω_{coup}^{ha} CBS [cm^{-1}]	ω_{coup} exp [cm^{-1}]
1	Σ	2365.1	2331	N2−N1	23.071	22.409	2365.1	2331.0	2.97	3.04	0.0	0.0
ZPE [kcal/mol]:		3.38	3.33				3.38				0.00	0.00
8, $[HNN]^+(^1\Sigma^+)$												
4	Σ	3442.6	3260	H3−N2	6.176	5.584	3339.0	3175.0	1.13 (0.89)	1.10 (0.87)	103.6	84.8
3	Σ	2313.2	2280	N2−N1	24.223	23.375	2423.2	2380.4	3.07	3.13	−110.1	−100.5
2	Π	730.3	714	H3−N2−N1	0.254	0.243	730.3	714.0			0.0	0.0
1	Π	730.3	714	H3−N2−N1	0.254	0.243	730.3	714.0			0.0	0.0
ZPE [kcal/mol]:		10.32	9.96				10.33	9.98			−0.01	−0.02
9, $[HNNH]^{2+}(^1\Sigma_g^+)$												
7	Σ_g	2994.8	2836	N2−H1	3.758	3.437	2604.8	2490.9	0.78 (0.61)	0.77 (0.61)	390.0	344.9
6	Σ_u	2592.1	2454	H4−N3	3.758	3.437	2604.8	2490.9	0.78 (0.61)	0.77 (0.61)	−12.6	−36.4
5	Σ_g	2198.8	2167	N3−N2	27.932	26.113	2602.1	2516.0	3.38	3.38	−403.3	−348.9
4	Π_u	800.8	783	N3−N2−H1	0.313	0.300	771.0	753.8			29.8	29.1
3	Π_u	800.8	783	H4−N3−N1	0.313	0.300	771.0	753.8			29.8	29.1
2	Π_g	753.5	737	N3−N2−H1	0.313	0.300	771.0	753.8			−17.5	−17.1
1	Π_g	753.5	737	H4−N3−N1	0.313	0.300	771.0	753.8			−17.5	−17.1
ZPE [kcal/mol]:		15.57	15.01				15.58	15.03			0.00	−0.02
10, $[CO]^+(^2\Sigma^+)$												
1	Σ	2305.0	2214	C1−O2	21.465	19.808	2305.0	2214.2	2.83	2.79	0.0	0.0
ZPE [kcal/mol]:		3.30	3.17				3.30	3.17			0.00	0.00
11, $[NO]^+(^1\Sigma^+)$												
1	Σ	2388.2	2376	N1−O2	25.091	24.844	2388.2	2376.4	3.15	3.26	0.0	0.0
ZPE [kcal/mol]:		3.41	3.40				3.41	3.40			0.00	0.00
19, $FCN(^1\Sigma^+)$												
4	σ	2364	2290	N3−C2	18.418	17.431	2199.4	2139.7	2.55	2.55	164.8	150.3
3	σ	1084	1078	C2−F1	8.780	8.589	1423.5	1407.9	1.45	1.51	−339.1	−329.9
2	π	460	451	N3−C2−F1	0.394	0.379	459.8	451.0			0.0	0.0
1	π	460	451	N3−C2−F1	0.394	0.379	459.8	451.0			0.0	0.0
ZPE [kcal/mol]:		0.66	0.64				0.66	0.64			0.00	0.00
20, $[FNNH]^{2+}(^1\Sigma^+)$												
7	σ	2834	2794	N3−N2	26.232	24.798	2521.7	2451.8	3.24	3.26	−168.7	341.7
6	σ	2353	2228	H4−N3	3.590	3.328	2545.7	2451.2	0.75	0.75	288.7	−223.1
5	σ	1100	1094	N2−F1	9.117	8.922	1385.4	1370.5	1.49	1.55	−285.5	−277
4	π	624	612	H4−N3−N2	0.197	0.19	611.1	599.3			12.7	12.7
3	π	624	612	H4−N3−N2	0.197	0.19	611.1	599.3			12.7	12.7
2	π	437	427	N3−N2−F1	0.365	0.349	442.0	432.1			−4.8	−4.7
1	π	437	427	N3−N2−F1	0.365	0.349	442.0	432.1			−4.8	−4.7
ZPE [kcal/mol]:		0.62	0.61				0.63	0.62			−0.01	−0.01
21, $[FNNF]^{2+}(^1\Sigma_g^+)$												
7	σ_g	2699	2661	N3−N2	25.475	24.817	2485.0	2452.8	3.18	3.26	214.4	207.8
6	σ_u	1270	1202	N2−F1	8.107	7.59	1306.4	1264.2	1.37	1.38	−36.7	−61.8

dx.doi.org/10.1021/jp406200w | J. Phys. Chem. A 2013, 117, 8981−8995

Table 2. continued

molecule μ	sym	ω_μ^{ha} CBS [cm^{-1}]	ω_μ exp [cm^{-1}]	parameter	κ_{ha}^a CBS [mdyn/Å]	k^a exp [mdyn/Å]	ω_{ha}^a BS [cm^{-1}]	ω^a exp [cm^{-1}]	n^{ha} CBS	n exp	ω_{coup}^{ha} CBS [cm^{-1}]	ω_{coup} exp [cm^{-1}]
5	σ_g	807	803	N2–F2	8.107	7.59	1306.4	1264.2	1.37	1.38	−499.0	−461.5
4	π_u	278	273	F4–N3–N2–F1	0.086	0.083	213.7	209.6			64.6	63.4
3	π_u	278	273	F4–N3–N2–F1	0.086	0.083	213.7	209.6			64.6	63.4
2	π_g	207	203	F4–N3–N2–F1	0.086	0.083	213.7	209.6			−6.4	−6.3
1	π_g	207	203	F4–N3–N2–F1	0.086	0.083	213.7	209.6			−6.4	−6.3
ZPE [kcal/mol]:		0.30	0.29				0.31	0.30			−0.01	−0.01

force constant is reduced from 18.6 by 17% to 15.5 mdyn/Å, which results in a RBSO of just 2.35. Hence protonation either can increase the bond strength to a fully developed triple bond or weaken it to become essentially a double bond.

In the case of the double protonation of CO, the bond strength of the CO bond is reestablished to meet triple bond character (n = 2.92, Table 2). Now, the atomic orbitals at the C and O atom are reduced in size as a result of two positive charges. The covalent radius of C and O is reduced, the bond length becomes smaller (1.156 Å or a 1% decrease, Figure 2), and overlap increases, thus causing an electronegativity-driven strengthening of the bond. It has been shown that an increase in bonding effectively counteracts destabilizing charge repulsion effects in dications[62−64] so that a kinetically stable but thermodynamically unstable system results. This is the case for $[HCOH]^{2+}(^1\Sigma^+)$, which dissociates to **2** or **3** in exothermic reactions (−67.9 and −33.0 kcal/mol, CCSD(T)/CBS, Figure 3) after surmounting barriers of 23.3 or 51.8 kcal/mol, respectively (CCSD(T)/CBS). Cations **2** and **3** are thermodynamically stable as reflected by proton affinities of 140.6 (protonation at C) and 102.4 kcal/mol (protonation at O, Table 5).

The XH RBSO values also listed in Tables 2 and 3 are given relative to the CH bond in methane (n = 1.00) and reflect the bond strength increase from the CH to NH and OH. We have also calculated the NH and OH RBSO values relative to the NH bond in NH_3 and the OH bond in H_2O as standard single bonds (given in parentheses in Tables 2 and 3). The latter values reveal that, with the exception of **2**, (double) protonation of CO leads to weak XH bonds.

Singly protonated CO was previously investigated by Dunning and co-workers.[65] These authors calculated accurate CCSD(T) values for various properties of $[HCO]^+$ and related molecules using up to aug-cc-pV5Z basis sets. Their results are in good agreement with our values. Grunenberg and co-workers[66] determined the strengthening (weakening) of the CO bond upon protonation at the C (O) atom where these authors used compliance constants for their analysis. Because compliance constants are the reciprocal of the local mode force constants (see above and references 10, 11, and 49; the local mode force constants were published 5 years before the investigation of Grunenberg and co-workers in 2003), their CCSD(T)/aug-cc-pVQZ results are in line with our CCSD(T)/CBS data. However, Grunenberg and co-workers did not rationalize the change in bond strength.[66]

Protonated isomers of carbon monoxide play important roles in terrestrial as well as extraterrestrial chemistry. Ion $[HCO]^+$ has been used as an example to explain bonding in cationic transition metal carbonyl complexes.[67,68] This ion was detected in interstellar space already in 1970[69] as was later its isomer $[COH]^+$.[70]

Protonation of Hydrogen Cyanide. $[HCNH]^+$ has been found to play a role in Titan's ionosphere.[71] Furthermore, it has been measured in dense molecular clouds of interstellar space via its electric quadrupole hyperfine structure.[72] Its relevance for the chemistry of long-term comets such as Hale-Bopp was discussed.[73]

Protonation at N has an electronegativity effect on the strength of the C≡N bond, which is not as unbalanced as in the case of the O-protonation of C≡O because the electronegativity difference between HC and N is smaller than that between C and O.[57] Thus, $[HCNH]^+(^1\Sigma^+)$ resembles more the double-protonated C≡O and possesses a bond similar to the triple bond (n = 2.87; k^a = 20.7 mdyn/Å, Table 2) of dinitrogen. Contrary to

dx.doi.org/10.1021/jp406200w | J. Phys. Chem. A 2013, 117, 8981−8995

Table 3. CCSD(T)/CBS and Experimental Normal and Local Mode Frequencies Frequencies, ω_μ and ω^a, Local Mode Force Constants, k^a, RBSO Values, n, and Coupling Frequencies, ω_{coup}, for Molecules 12−18

molecule μ	sym	ω_μ^{ha} CBS [cm^{-1}]	ω_μ exp [cm^{-1}]	parameter	κ_{ha}^a CB [mdyn/Å]	k^a exp [mdyn/Å]	ω_{ha}^a CBS [cm^{-1}]	ω^a exp [cm^{-1}]	n^{ha} CBS	n exp	ω_{coup}^{ha} CBS [cm^{-1}]	ω_{coup} exp [cm^{-1}]
12, $H_3COH(^1A')$												
12	A′	3884.7	3681	H6−O2	8.410	7.552	3880.1	3676.9	1.41 (1.02)	1.37 (0.99)	4.7	4.1
11	A′	3132.5	3000	H3−C1	5.337	4.882	3121.5	2985.3	1.01	1.00	11.0	14.7
10	A″	3114.1	2960	H5−C1	5.152	4.600	3066.8	2898.0	0.98	0.96	47.3	62.0
9	A′	3032.3	2844	H4−C1	5.152	4.600	3066.8	2898.0	0.98	0.96	−34.5	−54.0
8	A′	1518.1	1477	H5−C1−H4	0.722	0.684	1502.7	1462.4			15.4	14.6
7	A″	1515.7	1477	H4−C1−H3	0.713	0.678	1496.5	1459.0			19.2	18.0
6	A′	1487.1	1455	H5−C1−H4-H3	0.511	0.488	1483.2	1450.3			3.9	4.7
5	A′	1380.1	1345	H4−C1−H3−O2	0.661	0.633	1314.2	1286.7			65.9	58.3
4	A″	1187.3	1165	H3−C1−O2	0.987	0.930	1301.8	1263.3			−114.5	−98.3
3	A′	1104.9	1060	H6−O2−C1	0.746	0.709	1255.4	1224.0			−150.5	−164.0
2	A′	1039.5	1033	O2−C1	4.639	4.515	1071.6	1057.2	1.00	1.00	−32.1	−24.2
1	A″	266.5	200	H6−O2−C1−H3	0.025	0.014	311.3	234.3			−44.9	−34.3
ZPE [kcal/mol]:		32.40	31.02				32.70	31.30			−0.30	−0.28
13, $H_2CO(^1A^+)$												
6	B_2	3033.6	2843	H3−C1	4.875	4.326	2983.3	2810.3	0.94	0.91	50.3	32.8
5	A_1	2939.1	2783	H4−C1	4.875	4.326	2983.3	2810.3	0.94	0.91	−44.2	−27.8
4	A_1	1788.8	1746	O2−C1	12.876	12.260	1785.3	1742.1	2.00	2.00	3.5	4.0
3	A_1	1539.6	1500	H4−C1−H3	0.811	0.770	1582.2	1542.0			−42.5	−41.9
2	B_2	1277.0	1249	H3−C1−O2	1.098	1.048	1397.3	1364.8			−120.3	−115.8
1	B_1	1189.6	1167	H4−C1−H3−O2	0.296	0.285	1189.6	1167.3			0.0	0.0
ZPE [kcal/mol]:		16.82	16.14				17.04	16.35			−0.22	−0.21
14, $H_2NNH_2(^1A)$												
12	B	3604.6	3350	H4−N1	6.996	6.013	3553.9	3294.6	1.23 (0.97)	1.16 (0.91)	50.6	55.4
11	A	3602.2	3330	H6−N2	6.996	6.013	3553.9	3294.6	1.23 (0.97)	1.16 (0.91)	48.3	35.4
10	A	3497.4	3280	H5−N2	6.718	5.825	3482.6	3242.8	1.20 (0.94)	1.14 (0.90)	14.8	37.2
9	B	3491.7	3261	H3−N1	6.718	5.825	3482.6	3242.8	1.20 (0.94)	1.14 (0.90)	9.1	18.2
8	A	1695.3	1312	H4−N1−N2	0.825	0.550	1263.6	1031.5			431.8	280.5
7	B	1683.2	1275	H6−N2−N1	0.825	0.550	1263.6	1031.5			419.6	243.5
6	A	1342.3	1098	H3−N1−N2	0.811	0.532	1252.8	1014.9			89.5	83.1
5	B	1313.4	966	H5−N2−N1	0.811	0.532	1252.8	1014.9			60.7	−48.9
4	A	1129.9	933	H4−N1−N2−H3	0.279	0.207	1105.3	950.7			24.6	−17.7
3	B	1008.0	875	H6−N2−N1−H5	0.279	0.207	1105.3	950.7			−97.3	−75.7
2	A	848.6	780	N2−N1	4.182	3.176	1006.8	877.4	0.93	0.78	−158.2	−97.4
1	A	419.3	377	H5−N2−N1−H3	0.072	0.058	566.7	507.4			−147.4	−130.4
ZPE [kcal/mol]:		33.79	29.79				32.72	29.24			1.07	0.55
15, $HNNH(^1A_g)$												
6	B_u	3314.5	3128	H3−N1	6.025	5.404	3298.1	3123.6	1.10 (0.87)	1.08 (0.85)	16.4	4.4
5	A_g	3282.9	3120	H4−N2	6.025	5.404	3298.1	3123.6	1.10 (0.87)	1.08 (0.85)	−15.2	−3.6
4	A_g	1619.3	1583	N2−N1	10.700	10.199	1610.6	1572.4	1.76	1.76	8.7	10.6
3	A_g	1572.3	1529	H3−N1−N2	1.123	1.072	1463.6	1429.8			108.7	99.2
2	B_u	1347.9	1322	H4−N2−N1	1.123	1.072	1463.6	1429.8			−115.7	−107.8
1	A_u	1324.1	1286	H4−N2−N1−H3	0.473	0.446	1324.1	1286.0			0.0	0.0
ZPE [kcal/mol]:		17.81	17.11				17.81	17.11			0.00	0.00
16, $[HC]^+(^1\Sigma^+)$												
1	Σ	2838.6	2740	H2−C1	4.382	4.083	2838.6	2740.0	0.87	0.88	0.0	0.0
ZPE [kcal/mol]:		4.06	3.92				4.06	3.92			0.00	0.00
17, $[HN]^+(^1\Sigma^+)$												
1	Σ	3048.6	2922	H2−N1	5.111	4.695	3048.6	2922.0	0.98 (0.77)	0.97 (0.78)	0.0	0.0
ZPE [kcal/mol]:		4.36	4.18				4.36	4.18			0.00	0.00
18, $[HO]^+(^1\Sigma^+)$												
1	Σ	3168.6	3113	H2−O1	5.567	5.375	3168.6	3113.4	1.04 (0.75)	1.07 (0.77)	0.0	0.0
ZPE [kcal/mol:]		4.53	4.45				4.53	4.45			0.00	0.00

$[HCOH]^{2+}$, the cation $[HCNH]^+$ is stable with regard to proton loss at N (168.9 kcal/mol, Table 5).

Both C≡O and HC≡N benefit from the electronegativity effect caused by (double) protonation of the heteroatom(s) thus converting electron lone pairs into electron bonding pairs and increasing the bond strength by 13−16% to that of a real triple bond, which they do not possess in their neutral form. If such a bond strengthening can be achieved in a case where a true triple bond already exists, a stronger than triple bond should be generated.

Protonation of Molecular Nitrogen. Protonation of N_2 leads to a molecule isoelectronic and similar in electronic

dx.doi.org/10.1021/jp406200w | J. Phys. Chem. A 2013, 117, 8981−8995

Table 4. BDE (Including Zero-Point Energy Corrections) and BDH(298) Values Calculated at the G4 Level and Compared with Experimental BDH Values[a]

molecule	fragments	BDE [kcal/mol]	BDH (298 K) [kcal/mol]	BDH (exp) [kcal/mol]
1, $CO(^1\Sigma^+)$	$C(^3P) + O(^3P)$	257.4	258.0	257.3
2, $[HCO]^+(^1\Sigma^+)$	$HC^+(^3\Pi) + O(^3P)$	275.9	276.5	
	$HC^+(^1\Sigma^+) + O(^1D)$	293.2	293.8	
3, $[COH]^+(^1\Sigma^+)$	$HO(^2\Pi) + C^+(^2P)$	202.6	203.1	
4, $[HCOH]^{2+}(^1\Sigma^+)$	$HC^+(^3\Pi^+) + OH^+(^3\Sigma^-)$	86.7	87.3	
	$HC^+(^1\Sigma^+) + OH^+(^1\Delta)$	114.3	114.9	
5, $HCN(^1\Sigma^+)$	$HC(^4S) + N(^4S^1)$	240.7	241.3	245.1
6, $[HCNH]^+(^1\Sigma^+)$	$HC^+(^3\Pi) + NH(^3\Sigma)$	271.8	272.4	
7, $N_2(^1\Sigma_g^+)$	$N(^4S^1) + N(^4S^1)$	225.7	226.3	225.8
8, $[HNN]^+(^1\Sigma^+)$	$HN^+(^4\Sigma^-) + N(^4S)$	260.3	260.9	
	$HN^+(^2\Pi) + N(^2D)$	314.9	315.5	
9, $[HNNH]^{2+}(^1\Sigma_g^+)$	$HN^+(^2\Pi) + HN^+(^2\Pi)$	118.7	119.3	
10, $[CO]^+(^2\Sigma^+)$	$C^+(^2P) + O(^3P)$	192.1	192.7	192.7
11, $[NO]^+(^1\Sigma^+)$	$N^+(3P) + O(^3P)$	272.0	272.6	
12, $H_3COH(^1A^+)$	$H_3C\cdot(^2\Pi_u) + OH(^2\Pi)$	90.7	91.3	92.0
13, $H_2CO(^1A^+)$	$H_2C:(^3B_1) + O(^3P)$	178.8	179.4	180.6
14, $H_2NNH_2(^1A)$	$H_2N(^2B_1) + H_2N(^2B_1)$	64.3	64.9	66.2
15, $HNNH(^1A_g)$	$HN(^3\Sigma) + HN(^3\Sigma)$	121.6	122.2	121.6
20, $[HNNF]^{2+}(^1\Sigma^+)$	$HN^+(^4\Sigma^-) + FN^+(^4\Sigma^-)$	113.8	114.4	
	$HN^+(^2\Pi) + FN^+(^2\Pi)$	12.2	12.8	
21, $[FNNF]^{2+}(^1\Sigma_g^+)$	$FN^+(^4\Sigma^-) + FN^+(^4\Sigma^-)$	101.0	101.6	
	$FN^+(^2\Pi) + FN^+(^2\Pi)$	−101.6	−101.0	

[a]Experimental BDH values from ref 4.

Table 5. G4 Proton Dissociation Energies of Protonated Molecules Reflecting Their Stability[a]

molecule	state	reaction	ΔE_0 [kcal/mol]	ΔH (298 K) [kcal/mol]
2, $[HCO]^+$	$^1\Sigma^+$	$[HCO]^+ \rightarrow CO + H^+$	140.6	140.6
3, $[COH]^+$	$^1\Sigma^+$	$[HOC]^+ \rightarrow CO + H^+$	102.4	102.4
4, $[HCOH]^{2+}$	$^1\Sigma^+$	$[HCOH]^{2+} \rightarrow [HCO]^+ + H^+$	−71.7	−70.5
		$[HCOH]^{2+} \rightarrow [HOC]^+ + H^+$	−33.8	−33.8
6, $[HCNH]^+$	$^1\Sigma^+$	$[HCNH]^+ \rightarrow HCN + H^+$	168.9	168.9
8, $[HNN]^+$	$^1\Sigma^+$	$[NNH]^+ \rightarrow N_2 + H^+$	116.9	116.9
9, $[HNNH]^{2+}$	$^1\Sigma_g^+$	$[HNNH]^{2+} \rightarrow [HNN]^+ + H^+$	−58.5	−58.5

[a]Values correspond to the protonon affinity of the less charged or neutral molecule. ΔE_0 values include ZPE (zero-point energy) corrections.

structure to HCN. The NN stretching force constant (k^a(NN) = 23.4 mdyn/Å, Table 2) is 4% larger than that of N_2 (k^a(NN) = 22.4 mdyn/Å), which corresponds to an increase in the RBSO from 3.04 to 3.13. The BDH value of molecular nitrogen increases by 13% to 260.9 kcal/mol (Table 4).

Discussion of the CO protonation above shows that double protonation is more effective than single protonation when aiming at an electronegativity-driven strengthening of the bond because any difference in the effective electronegativities of the protonated and nonprotonated center leads to a decrease in overlap. As shown in Table 2, double-protonated N_2, which is isoelectronic with acetylene and protonated HCN, has the largest stretching force constant (k^a(NN) = 26.1 mdyn/Å) ever observed and by this a 16% larger bond strength than N_2 corresponding to a RBSO of 3.38. The CCSD(T)/CBS bond length is 1.080 Å and by this significantly shorter than that of N_2 (1.097 Å, Figure 2). A shortening of the bond length, however, does not necessarily indicate a strengthening of the bond. For example in the present case, protonation leads to a depletion of charge at N and a smaller covalent radius of the more positively charged N atom. Hence, the bond length depends in first order on the volume of the atom and in second order on the overlap, whereas the bond strength directly depends on the overlap.

The NH bonds formed upon (double) protonation are significantly weaker than a normal NH bond as is reflected by their relatively low NH stretching force constants and NH RBSO values of 0.87 (**8**) and 0.77 (**9**), respectively. The increase of the strength of the central bond implies that the NH bonds are weaker. Hence, the thermodynamical stability of $[HNNH]^{2+}$ is 58.5 kcal/mol smaller than that of $[HNN]^+$ (Table 5). The dication is, however, kinetically stable by 33.7 kcal/mol (Figure 3), which corresponds to the relative energy of the transition state of the proton loss reaction.

Comparing the three protonated triply bonded systems C≡O, HC≡N, and N≡N, the latter has clearly the strongest bond when doubly protonated. The strengthening is a result of the electronegativity-driven decrease of the energy of the bonding orbitals, which is most effective when it does not weaken orbital overlap; i.e., the bond should be between equal atoms as in dication **9**.

We also investigated the possibility of replacing protons by F^+ cations so that an even stronger NN bond can result. There is of course the question whether the generation of an extended π-conjugated system leads more to an equalization of the bond strength (the NF bond strength increasing, that of the NN bond decreasing). The π-MOs shown in Figure 4 reveal that the NN

dx.doi.org/10.1021/jp406200w | J. Phys. Chem. A 2013, 117, 8981−8995

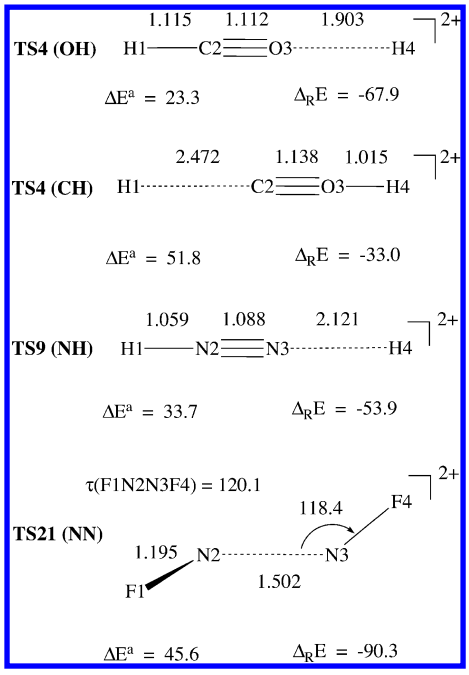

Figure 3. CCSD(T)/CBS geometries of the transition states **TS4(OH)**, **TS4(CH)**, **TS9(NH)**, and **TS21(NN)**. Bond lengths in Å and angles in deg. The numbering of atoms is indicated. Activation energies ΔE^a and reaction energies $\Delta_R E$ in kcal/mol calculated at the CCSD(T)/CBS level of theory using CCSD(T)/CBS geometries.

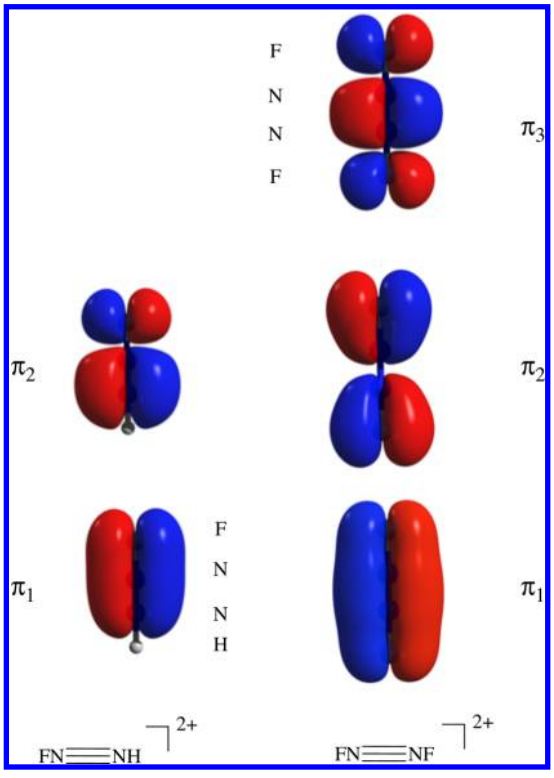

Figure 4. Occupied π-MOs of $[FNNH]^{2+}(^1\Sigma^+)$ and $[FNNF]^{2+}(^1\Sigma_g^+)$.

antibonding (bond weakening) MO π_2 is compensated by a NN bonding (strengthening) MO π_3, thus making it difficult to predict the NN bond strength of **21** on qualitative grounds.

Both $[FNNH]^+$ and $[FNNF]^{2+}$, which were previously discussed by Olah and co-workers,[63,64] possess a stronger bond than N_2 in its ground state; however, they reach only 90 and 97% of the strength of the NN bond in $[HNNH]^{2+}$. Clearly, the F substituents increase the electronegativity effect introduced by the two positive charges. However, at the same time π-electron withdrawal to the more electronegative F atoms and the establishment of NF bonds with partial double bond character (n = 1.38), leads to a weakening of the central bond (n = 3.26), which reduces the electronegativity effect (Table 2). This analysis has been verified by testing the dication $[XNNX]^{2+}$ with X being the electropositive substituent BeH. In this case, the NN bond strength is significantly reduced (by 0.78 relative to the RBSO of **9**), thus indicating that a decrease of the effective electronegativity of N (augmented by π-electron delocalization) leads to a weakening to the NN bond.

The cation $[FNNF]^{2+}$ is the only example investigated, for which the dissociation into two $NF(^2\Pi)$ molecules is exothermic (−101.6 kcal/mol, Table 4) whereas NN dissociation to NF molecules in their excited $^4\Sigma^-$ state is endothermic (101.0 kcal/mol; similar values for NN dissociation of $[FNNH]^+$; Table 4). However, **21** is kinetically stable because of a large barrier of 45.6 kcal/mol calculated at the CCSD(T)/CBS level of theory (Figure 3). Noteworthy is that the linear dication adopts a gauche transition state conformation with a dihedral angle FNNF of 120° and a FNN angle of 118°. The unusual transition state geometry results from the fact that during dissociation there is a rehybridization at the N atoms to $sp^2-p\pi$ where the NF bonding electron pair, the N electron lone pair, and an unpaired electron occupy the sp^2-hybrid orbitals and the higher lying $p\pi$-orbital is empty. This leads to a trans- or cis-structure. The C_2-symmetrical gauche-structure minimizes lone pair-bond pair electron repulsion and therefore is more stable than the planar structures.

After discussing an electronegativity increase because of protonation or substitution, we will discuss in the following the question whether an electronegativity-driven strengthening of the bond can also be enforced by ionization.

Cations $[CO]^+$ and $[NO]^+$. One could consider many possibilities of bond strengthening via ionization; however, the lesson learned from the protonation examples discussed above limits the number of promising molecules for such an investigation. First of all, ionization will only lead to bond strengthening when an antibonding or lone pair electron rather than a bonding electron is ionized. Hence, N_2 is not a suitable candidate for an ionization-driven bond strengthening because its HOMO is a π-bonding orbital. Second, ionization of a heterolytic bond AB must occur at the less electronegative center to avoid an increase in the electronegativity difference and thereby a weakening of bonding overlap.

Ionization of carbon monoxide involves the lone pair electron at C and therefore should lead to a stronger bond for the doublet radical $[CO]^+(^2\Sigma^+)$. The data in Table 2 confirm this: The local stretching force constant is larger than that of the parent molecule CO (21.5 vs 19.1 mdyn/Å) and the RBSO increases to 2.79, which is closer to a fully developed triple bond but not establishing the strength of a triple bond.

The ionization of an antibonding electron should be more effective and in this connection the nitric oxide radical is a suitable candidate because it has an unpaired electron in the π-antibonding orbital. The latter has a large coefficient at N, and therefore, ionization of the unpaired electron leads to a more positively charged N with an effective electronegativity that should be close to that of the O atom. This assumption is confirmed by a large $[N\equiv O]^+$ stretching force constant of 25.1 mdyn/Å and a RBSO of 3.26, which is identical to that of $[FNNF]^{2+}$ (Table 2).

dx.doi.org/10.1021/jp406200w | J. Phys. Chem. A 2013, 117, 8981−8995

Other systems such as $[HCO]^{2+}$ (n = 1.9 because ionization is from a bonding MO) or $[HNN]^{2+}$ (n = 3.1) do not lead to stronger bonds than found for $[HNNH]^{2+}$, although bond strengthening is also observed in the second case. Clearly, ionization cannot help in the cases of HC≡CH for the reasons described but will work in the case of C═C($^1\Sigma_g^+$) or C≡N($^1\Sigma_g^+$).

Bond Dissociation Energies Are Not Reliable Bond Strength Descriptors. BDE or BDH values are standard means to assess the strength of the chemical bond.[4,7] They measure the energy (enthalpy) difference between the dissociating molecule at its equilibrium geometry in the ground state and the fragment energies (enthalpies) in their equilibrium geometry. In Figure 5, the dissociation curves of $[HCO]^+$ and $[HNN]^+$ are schematically shown.

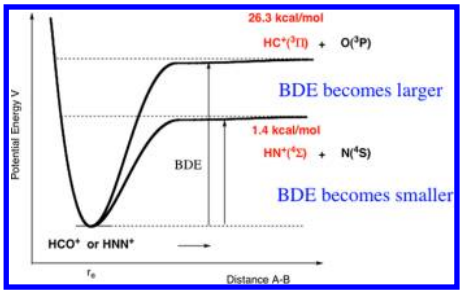

Figure 5. Schematic representation of a bond dissociation energy (BDE) for a dissociation yielding a fragment in a high-lying excited state ($[HCO]^+(^1\Sigma^+)$; large BDE) or low-lying excited state ($[HNN]^+(^1\Sigma^+)$; small BDE). Relative excited state energies are taken from experiment[43,52] and are indicated in red.

Dissociation of a cation $[AB]^+$ will normally take place in the way that the positive charge stays with the atom or group having the smallest effective electronegativity. In the case of cations **2** and **8**, these would be the groups HC and HN, respectively. There must be a conservation of spin; i.e., the singlet state of $[HCO]^+$ must dissociate either to two singlet or to two triplet states, as indicated in Figure 5. This implies that always one of the fragments is formed in an excited state and that the stability of the excited state influences the magnitude of the BDE. The first excited state of the $[HC]^+$ ion is a $^3\Pi$ state and 26.3 kcal/mol above the corresponding $^1\Sigma^+$ ground state[43] whereas the first excited state of the O atom is a ^{1}D state and 45.4 kcal/mol above the ^{3}P ground state.[43] Clearly, the energetically favorable dissociation of $[HCO]^+(^1\Sigma^+)$ leads to $[HC]^+(^3\Pi)$ and O(^{3}P) as is confirmed by the BDEs of Table 4 (275.9 compared to 293.2 kcal/mol).

We conclude that the BDE measures both the stability of the excited state and the bond strength. If there is a suitable low-lying excited state, the BDE will be relatively small and falsely suggests that the bond strength is low. An example is the dissociation of $[HNN]^+(^1\Sigma^+)$, also shown in Figure 5. Dissociation into two doublet states, $[HN]^+(^2\Pi)$ and N(^{2}D), requires 315 kcal/mol (Table 4) and is unlikely. Dissociation into two quartet states, $[HN]^+(^4\Sigma)$ and N(^{4}S), requires only 260.3 kcal/mol, which is a direct result of the fact that the $[HN]^+(^4\Sigma)$ state is just 1.4 kcal/mol above the $[HN]^+(^2\Pi)$ ground state.[43] Hence, by comparing the BDEs of $[HCO]^+$ and $[HNN]^+$ (275.9 and 260.3 kcal/mol, Table 4) and falsely using them as bond strength descriptors, one would draw the wrong conclusion that the CO bond is stronger than the NN bond in these cations.

The situation is even more contradictory in the case of the $[HNNH]^{2+}(^1\Sigma_g^+)$ ion, which dissociates to two $[HN]^+(^2\Pi)$ ions characterized by a BDE value of just 118.7 kcal/mol. This is due to the stability of the $[HN]^+$ cation and not a reflection of a low NN bond strength. One might argue that the NN bond is weakened by two positive charges. However, these charges are largely localized at the H atoms and do not lead to a direct destabilizing Coulomb repulsion. The low BDE value is more a direct result of the high relaxation energy of the two fragments: The NH cations have a geometry (1.069 vs 1.095 Å, Figure 2) and electronic structure significantly different from that of the NH groups in $[HNNH]^{2+}$. Hence, they strongly stabilize themselves via electron and geometry reorganization, which leads to a substantial lowering of the BDE. A similar effect is observed for $[HCOH]^{2+}$, which also has a low BDE of just 86.7 kcal/mol when dissociating to $[HC]^+(^3\Pi^+)$ + $[OH]^+(^3\Sigma^-)$ and 114.3 kcal/mol when dissociating to $[HC]^+(^1\Sigma^+)$ + $[OH]^+(^1\Delta)$.

4. WHAT IS THE STRONGEST BOND IN CHEMISTRY?

As shown in the previous section, BDEs are unreliable descriptors of the bond strength because they depend on both the stability of the dissociation products and the strength of the bond being cleaved. Therefore, it is not possible to determine via BDE values the strongest bond in chemistry. However, the strength of a bond can be reliably determined by the dynamic measure of the local bond stretching force constant k^a. A local stretching mode probes the strength of a bond where the stretching force constant corresponds to an infinitesimal change of the bond, which does not lead to any relevant change in the electronic structure of the bond.

In Figure 6, the RBSO n of the triple bonds investigated in this work are given as a function of the local stretching force constant

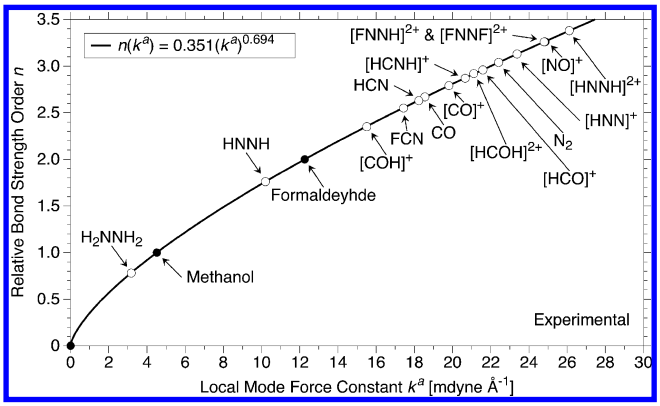

Figure 6. Relationship between RBSO values n(AB) and local mode stretching force constants k^a(AB) according to experimental frequencies (where available) or scaled CCSD(T)/CBS frequencies. The reference points (indicated by black dots) for the power relationship n = $0.351(k^a)^{0.694}$ are the C−O bond of methanol (n = 1.0), the C═O bond of formaldehyde (n = 2.0), and n = 0 for k^a(AB) = 0.

k^a where the latter is based on measured normal-mode frequencies or scaled CCSD(T)/CBS vibrational frequencies. Also shown are the reference molecules methanol and formaldehyde and their NN-analogues hydrazine and *trans*-diazene. The latter have weaker bonds than their isoelectronic CO counterparts. This is a result of lone pair-lone pair repulsion leading to RBSO values of n = 0.78 and 1.76 (Table 3). One could come to the same conclusion by taking the ratios of the calculated (or measured) BDE (BDH) values. However, in this connection one must not overlook that the BDEs are also determined by the stabilities of HN($^3\Sigma^-$) and $H_2N(^2B_1)$.

dx.doi.org/10.1021/jp406200w | J. Phys. Chem. A 2013, 117, 8981−8995

The focus on the protonation of triple-bond molecules involving either a N or O atom was based on the following rules: (i) Because of hybridization and overlap the strongest bond will be formed by elements of the second period. (ii) The reference bond AB must be a triple or close to a triple bond. (iii) Bond strengthening must be generated by an electronegativity increase of the atoms forming the triple bond. (iv) An equal electronegativity increase for a homolytic bond AA is more effective than an unbalanced electronegativity increase of a heterolytic bond AB. (v) An electronegativity increase by protonation is more effective than that caused by ionization because the former withdraws two lone pair electrons whereas the latter can remove only one lone pair electron. However, when an antibonding electron is ionized, a strong effect can also be accomplished. (vi) Using F^+ ions instead of protons leads also to strong AA triple bonds; however, it is not as effective as protonation because density is drawn into the FA bond.

The changes in the bond strength caused by an electronegativity increase have been quantified with the local bond stretching force constants derived from experimental or scaled CCSD(T)/CBS frequencies. For the molecules investigated, stretching force constants with values between 21.0 and 26.1 mdyn/Å corresponding to RBSO values between 2.96 and 3.38 have been determined.

Molecules such as CO and HCN, which formally possess triple bonds, have weaker heavy atom bonds than for example N_2 but come close to fully developed triple bonds upon protonation at N or C or double-protonation as in the case of CO. The only bonds being stronger than triple bonds are found for $[HNN]^+(^1\Sigma^+)$, $[NO]^+(^1\Sigma^+)$, and $[HNNH]^{2+}(^1\Sigma_g^+)$, which are isoelectronic with HCN, NN, and HCCH, respectively. They are examples for an electronegativity-driven bond strengthening caused either by protonation at a lone pair side or by ionization of an antibonding electron. No other second period bond AB was found to have a larger stretching force constant and RBSO.

According to our investigations, the strongest bond in chemistry is the NN bond of the $[HNNH]^{2+}(^1\Sigma_g^+)$ molecule, which has an NN stretching force constant of 26.1 mdyn/Å, a bond length of 1.080 Å, and a RBSO of 3.38, which clearly exceeds the strongest triple bond of protonated CO or HCN. The doubly protonated dinitrogen is an example for a dication, which are discussed in chemistry for more than 40 years.[62,63,74,75] $[HNNH]^{2+}$ can be formed in diazonium reactions.[64] Its singly protonated analogue, $[NNH]^+$, was invoked as an intermediate in the diazotization of ammonia.[75] Clustering reactions of $[NNH]^+$ with molecular hydrogen were investigated in the gas phase.[76] Together with $[HNNH]^{2+}$, it is of direct relevance for extraterrestrial chemistry.[77] As pointed out above, none of the triple-bonded ions investigated in this work can be considered as an exotic species, which makes the discussion of the strength of their heavy atom bond relevant.

Finally, it has to be emphasized that by quantifying the strength of triple bonds via RBSO values we do not intend to redefine bond multiplicity in chemistry. It is useful to formally define the CC bond of acetylene as a triple bond compared to the CC bonds in ethane and ethene. Our investigation confirms this description. However, when it comes to comparing CC and NN triple bonds, the strength of the latter is substantially larger as reflected by RBSO values of 3.04 and 2.39, which is a direct consequence of the electronegativity influence on the bond strength. Future work will focus on the derivation of bond energy scales to relate RBSO values to energies.

This work has also shown an interesting dissociation behavior of linear $[FNNF]^{2+}$, which proceeds via a barrier of 45.6 kcal/mol and a gauche form characterized by a dihedral angle of 120°. An explanation for this unusual structure change has been given in this work.

■ ASSOCIATED CONTENT

Supporting Information

Calculated CCSD(T) frequencies, decomposition of normal vibrationmal modes into local vibrational modes, NBO charges, adiabatic connection schemes, and CCSD(T) geometries. This material is available free of charge via the Internet at http://pubs.acs.org.

■ AUTHOR INFORMATION

Corresponding Author

*D. Cremer: e-mail, dieter.cremer@gmail.com.

Notes

The authors declare no competing financial interest.

■ ACKNOWLEDGMENTS

This work was financially supported by the National Science Foundation, Grant CHE 1152357. We thank SMU for providing computational resources.

■ REFERENCES

(1) Pauling, L. *The Nature of the Chemical Bond*; Cornell University Press: Ithaca, NY, 1960.
(2) Slater, J. C. Directed Valence in Polyatomic Molecules. *Phys. Rev.* **1931**, *37*, 481−489.
(3) Mulliken, R. S. Overlap Integrals and Chemical Binding1. *J. Am. Chem. Soc.* **1950**, *72*, 4493−4503.
(4) Luo, Y.-R. *Comprehensive Handbook of Chemical Bond Energies*; Taylor and Francis: Boca Raton, FL, 2007.
(5) Schmidt, M. W.; Truong, P. N.; Gordon, M. S. π-Bond Strengths in the Second and Third Periods. *J. Am. Chem. Soc.* **1987**, *109*, 5217−5227.
(6) Schmidt, M. W.; Gordon, M. S. π-Bond Strengths in HP═PH, H_2P═P, HP═NH, and HN═NH. *Inorg. Chem.* **1986**, *25*, 248−254.
(7) Lide, D. R. E. *CRC Handbook of Chemistry and Physics on CD-ROM*; CRC Press LLC: Boca Raton, FL, 2000.
(8) Pyykkö, P.; Riedel, S.; Patzschke, M. Triple-Bond Covalent Radii. *Chem.—Eur. J.* **2005**, *11*, 3511−3520.
(9) Cremer, D.; Wu, A.; Larsson, A.; Kraka, E. Some Thoughts About Bond Energies, Bond Lengths, and Force Constants. *J. Mol. Model.* **2000**, *6*, 396−412.
(10) Zou, W.; Kalescky, R.; Kraka, E.; Cremer, D. Relating Normal Vibrational Modes to Local Vibrational Modes With the Help of an Adiabatic Connection Scheme. *J. Chem. Phys.* **2012**, *137*, 084114-1−084114-11.
(11) Zou, W.; Kalescky, R.; Kraka, E.; Cremer, D. Relating Normal Vibrational Modes to Local Vibrational Modes Benzene and Naphthalene. *J. Mol. Model.* **2012**, 1−13.
(12) Cremer, D.; Larsson, J. A.; Kraka, E. In *New Developments in the Analysis of Vibrational Spectra on the Use of Adiabatic Internal Vibrational Modes*; Parkanyi, C., Ed.; Elsevier: Amsterdam, 1998; p 259.
(13) Kraka, E.; Larsson, J. A.; Cremer, D. In *Generalization of the Badger Rule Based on the Uses of Adiabatic Vibrational Modes*; Grunenberg, J., Ed.; Wiley: New York, 2010; p 105.
(14) Cremer, D.; Kraka, E. From Molecular Vibrations to Bonding, Chemical Reactions, and Reaction Mechanism. *Curr. Org. Chem.* **2010**, *14*, 1524−1560.
(15) Badger, R. M. A Relation Between Internuclear Distances and Bond Force Constants. *J. Chem. Phys.* **1934**, *2*, 128−131.
(16) Decius, J. C. Compliance Matrix and Molecular Vibrations. *J. Chem. Phys.* **1963**, *38*, 241−248.

(17) Brandhorst, K.; Grunenberg, J. How Strong is it? The Interpretation of Force and Compliance Constants as Bond Strength Descriptors. *Chem. Soc. Rev.* **2008**, *37*, 1558−1567.
(18) Vijay Madhav, M.; Manogaran, S. A Relook at the Compliance Constants in Redundant Internal Coordinates and Some New Insights. *J. Chem. Phys.* **2009**, *131*, 174112-1−174112-6.
(19) Grunenberg, J.; Goldberg, N. How Strong Is the Gallium≡Gallium Triple Bond? Theoretical Compliance Matrices as a Probe for Intrinsic Bond Strengths. *J. Am. Chem. Soc.* **2000**, *122*, 6045−6047.
(20) Brandhorst, K.; Grunenberg, J. Efficient Computation of Compliance Matrices in Redundant Internal Coordinates From Cartesian Hessians for Nonstationary Points. *J. Chem. Phys.* **2010**, *132*, 184101-1−184101-7.
(21) Espinosa, A.; Streubel, R. Computational Studies on Azaphosphiridines, or How to Effect Ring-Opening Processes through Selective Bond Activation. *Chem.—Eur. J.* **2011**, *17*, 3166−3178.
(22) McKean, D. C. Individual CH Bond Strengths in Simple Organic Compounds: Effects of Conformation and Substitution. *Chem. Soc. Rev.* **1978**, *7*, 399−422.
(23) Duncan, J. L.; Harvie, J. L.; McKean, D. C.; Cradock, C. The Ground-State Structures of Disilane, Methyl Silane and the Silyl Halides, and An SiH Bond Length Correlation with Stretching Frequency. *J. Mol. Struct.* **1986**, *145*, 225−242.
(24) Murphy, W. F.; Zerbetto, F.; Duncan, J. L.; McKean, D. C. Vibrational-Spectrum and Harmonic Force-Field of Trimethylamine. *J. Phys. Chem.* **1993**, *97*, 581−595.
(25) Henry, B. R. The Local Mode Model and Overtone Spectra: A Probe of Molecular Structure and Conformation. *Acc. Chem. Res.* **1987**, *20*, 429−435.
(26) Konkoli, Z.; Cremer, D. A New Way of Analyzing Vibrational Spectra. I. Derivation of Adiabatic Internal Modes. *Int. J. Quantum Chem.* **1998**, *67*, 1−9.
(27) Wilson, E. B.; Decius, J. C.; Cross, P. C. *Molecular Vibrations. The Theory of Infrared and Raman Vibrational Spectra*; McGraw-Hill: New York, 1955.
(28) Kalescky, R.; Zou, W.; Kraka, E.; Cremer, D. Local Vibrational Modes of the Water Dimer - Comparison of Theory and Experiment. *Chem. Phys. Lett.* **2012**, *554*, 243−247.
(29) Kalescky, R.; Kraka, E.; Cremer, D. Local Vibrational Modes of the Formic Acid Dimer − The Strength of the Double H-Bond. *Mol. Phys.*, in press
(30) Konkoli, Z.; Larsson, J.; Cremer, D. A New Way of Analyzing Vibrational Spectra. II. Comparison of Internal Mode Frequencies. *Int. J. Quantum Chem.* **1998**, *67*, 29−40.
(31) Dunning, T. H. Gaussian Basis Sets for use in Correlated Molecular Calculations. *J. Chem. Phys.* **1989**, *90*, 1007−1023.
(32) He, Y.; Cremer, D. Molecular Geometries at Sixth Order Möller-Plesset Perturbation Theory. At What Order Does MP Theory Give Exact Geometries? *J. Phys. Chem. A* **2000**, *104*, 7679−7688.
(33) Cremer, D.; Kraka, E.; He, Y. Exact Geometries from Quantum Chemical Calculations. *J. Mol. Struct.* **2001**, *567*, 275−293.
(34) Dollish, F. R.; Fately, W. G.; Bentley, F. F. *Characteristic Raman Frequencies of Organic Compounds*; Wiley: New York, 1974.
(35) Puzzarini, C.; Tarroni, R.; Palmieri, P.; Carter, S.; Dore, L. Accurate ab Initioprediction of the Equilibrium Geometry of HCO+ and of Rovibration Energy Levels of DCO+. *Mol. Phys.* **1996**, *87*, 879−898.
(36) Pichierri, F. Theoretical Study of the Proton Exchange Reaction: $HCNH^+ + HCN \leftrightarrow HNC + HCNH^+$. *Chem. Phys. Lett.* **2002**, *353*, 383−388.
(37) Altman, R. S.; Crofton, M. W.; Oka, T. HIgh Resolution Infrared Spectroscopy of the ν_1 (NH Stretch) and ν_2 (CH Stretch) Bands Of $HCNH^+$. *J. Chem. Phys.* **1984**, *81*, 4255.
(38) Altman, R. S.; Crofton, M. W.; Oka, T. Observation of the Infrared ν_2 Band (CH Stretch) of Protonated Hydrogen Cyanide, HCNH+. *J. Chem. Phys.* **1984**, *80*, 3911−3912.
(39) Tanaka, K.; Kawaguchi, K.; Hirota, E. Diode Laser Spectroscopy of the ν_4 (HCN Bend) Band of $HCNH^+$. *J. Mol. Spectrosc.* **1986**, *117*, 408−415.
(40) Kajita, M.; Kawaguchi, K.; Hirota, E. Diode Laser Spectroscopy of the ν_3 (CN Stretch) Band Of HCNH+. *J. Mol. Spectrosc.* **1988**, *127*, 273−276.
(41) Ho, W.-C.; Blom, C. E.; Liu, D.-J.; Oka, T. The Infrared ν_5 Band (HNC Bend) of Protonated Hydrogen Cyanide, $HCNH^+$. *J. Mol. Spectrosc.* **1987**, *123*, 251−253.
(42) Crawford, M. F.; Welsh, H. L.; Locke, J. L. Infra-Red Absorption Of Oxygen And Nitrogen Induced By Intermolecular Forces. *Phys. Rev.* **1949**, *75*, 1607−1609.
(43) Herzberg, G.; Huber, K. P. *Molecular Spectra and Molecular Structure. IV. Constants of Diatomic Molecules*; Van Nostrand, Reinhold: New York, 1979; Vol. *1*
(44) Shimanouchi, T. *Tables of Molecular Vibrational Frequencies Consolidated*; National Bureau of Standards, 1972; Vol. *I*.
(45) Machado, F. B.; Roberto-Neto, O. An ab Initio Study of the Equilibrium Geometry and Vibrational Frequencies of Hydrazine. *Chem. Phys. Lett.* **2002**, *352*, 120−126.
(46) Craig, N. C.; Levin, I. W. Vibrational Assignment and Potential Function for *trans*-Diazene (Diimide): Predictions for *cis*-Diazene. *J. Chem. Phys.* **1979**, *71*, 400−407.
(47) Fawcett, F. S.; Lipscomb, R. D. Cyanogen Fluoride: Synthesis and Properties. *J. Am. Chem. Soc.* **1964**, *86*, 2576−2579.
(48) Kraka, E.; Cremer, D. Characterization of CF Bonds with Multiple-Bond Character: Bond Lengths, Stretching Force Constants, and Bond Dissociation Energies. *ChemPhysChem* **2009**, *10*, 686−698.
(49) Freindorf, M.; Kraka, E.; Cremer, D. A Comprehensive Analysis of Hydrogen Bond Interactions Based on Local Vibrational Modes. *Int. J. Quantum Chem.* **2012**, *112*, 3174−3187.
(50) Kawaguchi, K.; Hirota, E. Diode Laser Spectroscopy of the ν_3 and ν_2 Bands of FHF^- in 1300 cm^{-1} Region. *J. Chem. Phys.* **1987**, 6838−6841.
(51) Curtiss, L. A.; Redfern, P. C.; Raghavachari, K. Gaussian-4 Theory. *J. Chem. Phys.* **2007**, *126*, 084108−084108−12.
(52) Moore, C. E. In *Tables of Spectra of Hydrogen, Carbon, Nitrogen, and Oxygen*; Gallagher, J. W., Ed.; CRC Press, Inc.: Boca Raton, FL, 1993.
(53) Spyromilio, J. Wave lengths of the [N ii] ^3P - ^1D forbidden lines. *Mon. Not. R. Astron. Soc.* **1995**, *277*, L59−L62.
(54) Kraka, E.; Filatov, M.; Zou, W.; Grafenstein, J.; Izotov, D.; Gauss, J.; He, Y.; Wu, A.; Polo, V.; Olsson, L.; Konkoli, Z.; He, Z.; Cremer, D. *COLOGNE2013*; Southern Methodist University: Dallas, TX, 2013.
(55) Stanton, J. F.; Gauss, J.; Harding, M. E.; Szalay, P. G.; et al. *CFOUR*, 2010; see http//www.cfour.de.
(56) Frisch, M.; et al. *Gaussian 09*, Revision A.1; Gaussian Inc.: Wallingford, CT, 2009.
(57) Porterfield, W. W. *Inorganic Chemistry, A Unified Approach*; Academic Press: San Diego, 1993.
(58) Burger, H.; Schneider, W.; Sommer, S.; Thiel, W.; Willner, H. The Vibrational Spectrum and Rotational Constants of Difluoroethyne FC 3/4 CF. Matrix and High Resolution Infrared Studies and ab Initio Calculations. *J. Chem. Phys.* **1991**, *95*, 5660−5670.
(59) Breidung, J.; Schneider, W.; Thiel, W.; Lee, T. The Vibrational Frequencies of Difluoroethyne. *J. Chem. Phys.* **1992**, *97*, 3498−3499.
(60) Koch, W.; Frenking, G.; Gauss, J.; Cremer, D.; Collins, J. R. Helium Chemistry: Theoretical Predictions and Experimental Challenge. *J. Am. Chem. Soc.* **1987**, *109*, 5917−5934.
(61) Frenking, G.; Koch, W.; Reichel, F.; Cremer, D. Light Noble Gas Chemistry: Structures, Stabilities, and Bonding of Helium, Neon and Argon Compounds. *J. Am. Chem. Soc.* **1990**, *112*, 4240−4256.
(62) Dunitz, T. K.; Ha, T. K. Non-Empirical SCF Calculations on Hydrogen-Like Molecules: the Effect of Nuclear Charge on Binding Energy and Bond Length. *J. Chem. Soc., Chem. Commun.* **1972**, *1972*, 568−569.
(63) Dunitz, T. K.; Ha, T. K. Gitonic Protodiazonium and Bisdiazonium Dications and their Role in Superacid Chemistry. *J. Am. Chem. Soc.* **1994**, *116*, 8985−8990.
(64) Olah, G. A.; Prakash, G. K. S.; Molnar, A.; Sommer, J. *Superacid Chemistry*; Wiley: Hoboken, NJ, 2009.

(65) Mourik, T.; Dunning, T.; Peterson, K. A. Ab Initio Characterization of the HCOx (x = −1, 0, +1) Species: Structures, Vibrational Frequencies, CH Bond Dissociation Energies, and HCO Ionization Potential and Electron Affinity. *J. Phys. Chem. A* **2000**, *104*, 2287−2293.
(66) Grunenberg, J.; Streubel, R.; von Frantzius, G.; Marten, W. The Strongest Bond in the Universe? Accurate Calculation of Compliance Matrices for the Ions N_2H^+, HCO^+, and HOC^+. *J. Chem. Phys.* **2003**, *119*, 165−169.
(67) Goldman, A. S.; Krogh-Jespersen, K. Why Do Cationic Carbon Monoxide Complexes Have High C-O Stretching Force Constants and Short C-O Bonds? Electrostatic Effects, Not σ-Bonding. *J. Am. Chem. Soc.* **1996**, *118*, 12159−12166.
(68) Lupinetti, A. J.; Fau, S.; Frenking, G.; Strauss, S. H. Theoretical Analysis of the Bonding Between CO and Positively Charged Atoms. *J. Phys. Chem. A* **1997**, *101*, 9551−9559.
(69) Buhl, D.; Snyder, L. E. Unidentified Interstellar Microwave Line. *Nature* **1970**, *228*, 267−269.
(70) Ziurys, L. M.; Apponi, A. J. Confirmation of Interstellar HOC^+: Reevaluating the $[HCO^+]/[HOC^+]$ Abundance Ratio. *Astrophys. J. Lett.* **1995**, *455*, L73−L76.
(71) Cravens, T. E.; et al. Composition of Titan's Ionosphere. *Geophys. Res. Lett.* **2006**, *33*, L07105−1−L07105−4.
(72) Ziurys, L. M.; Apponi, A. J.; Yoder, J. T. Detection of the Quadrupole Hyperfine Structure in HCNH(+). *Astrophys. J. Lett.* **1992**, *397*, L123−L126.
(73) Ziurys, L. M.; Savage, C.; Brewster, M. A.; Apponi, A. J.; Pesch, T. C.; Wyckoff, S. Cyanide Chemistry in Comet Hale-Bopp (C/1995 O1). *Astrophys. J. Lett.* **1999**, *527*, L67−L71.
(74) Gill, P. M.; Radom, L. Structures and Stabilities of the Dimer Dications of First-and Second-Row Hydrides. *J. Am. Chem. Soc.* **1989**, *111*, 4613−4622.
(75) Olah, G. A.; Herges, R.; Felberg, J. D.; Prakash, G. S. Intermediacy of the Parent Diazonium Ion (Protonated Dinitrogen, N_2^+H) in the Diazotization of Ammonia and its Derivatives With $^{15}NO^+BF_4^-$ Giving $^{15}N^{14}N^+$. *J. Am. Chem. Soc.* **1985**, *107*, 5282−5283.
(76) Hiraoka, K. Clustering Reactions of the Protonated Nitrogen N_2H^+ With Hydrogen Molecule in the Gas Phase. *Bull. Chem. Soc. Jpn.* **1979**, *52*, 1578−1582.
(77) Caselli, P.; Myers, P. C.; Thaddeus, P. Radio-Astronomical Spectroscopy of the Hyperfine Structure of N_2H^+. *Astrophys. J. Lett.* **1995**, *455*, L77−L80.